

Electro-oxidation of ethylene glycol on PtRu/C and PtSn/C electrocatalysts prepared by alcohol-reduction process

A.O. NETO*, T.R.R. VASCONCELOS, R.W.R.V. DA SILVA, M. LINARDI and E.V. SPINACÉ
Instituto de Pesquisas Energéticas e Nucleares – IPEN/CNEN-SP, Centro de Ciência e Tecnologia de Materiais, Av. Prof. Lineu Prestes, 2242, Cidade Universitária, 05508-900, São Paulo- SP, Brazil
(*author for correspondence, fax: +55-11-3816-9440, e-mail: aolivei@ipen.br; espinace@ipen.br)

Received 29 June 2004; accepted in revised form 27 October 2004

Key words: alcohol-reduction process, electro-oxidation, ethylene glycol, fuel cell, PtRu/C, PtSn/C

Abstract

PtRu/C and PtSn/C electrocatalysts were prepared by the alcohol-reduction process with different atomic ratios. The electrocatalysts were characterized by EDAX, XRD, TEM and cyclic voltammetry and the electro-oxidation of ethylene glycol was studied by cyclic voltammetry and chronoamperometry using the thin porous coating technique. PtRu/C and PtSn/C electrocatalysts were found to be active for ethylene glycol oxidation, which starts at lower potentials by increasing the ruthenium and tin content. In the region of interest for direct alcohol fuel cell applications PtSn/C electrocatalysts were more active than PtRu/C electrocatalysts.

1. Introduction

Fuel Cells employing alcohols directly as fuel (Direct Alcohol Fuel Cell – DAFC) are extremely attractive as power sources for mobile, stationary and portable applications. The alcohol is fed directly into the fuel cell without any previous chemical modification and is oxidized at the anode while oxygen is reduced at the cathode. This avoids the problems related to production, purification and storage of hydrogen. However, alcohols are very difficult to electrooxidize completely, which results in products like aldehydes and acids [1–5].

Methanol has been considered the most promising organic fuel because it is more efficiently oxidized than other alcohols; on the other hand, it is toxic and the methanol crossover through the polymer-electrolyte membrane results in a decrease of efficiency [6–8].

Ethanol is a renewable and attractive fuel as it can be produced in large quantities from biomass and it is much less toxic than methanol. Until now, however, in direct ethanol fuel cells it cannot be completely oxidized to CO₂, acetaldehyde and acetic acid being the principal products formed [9, 10].

Recently, Peled et al. [11, 12] reported that methanol/oxygen and ethylene glycol/oxygen fuel cells equipped with a new nanoporous proton-conducting membrane and using PtRu/C (atomic ratio of 1:1) as anode catalyst provided a maximum power density of 400 and 300 mW cm⁻², respectively, which puts ethylene glycol in direct competition with methanol as a promising candidate for practical electric vehicles and stationary

applications [12]. Kelaidopoulou et al. [13] observed that the addition of ruthenium and tin onto platinum dispersed in polyaniline increases the electro-oxidation of ethylene glycol in acid medium; however, the influence of PtRu or PtSn composition was not investigated. Based on these results, Vielstich et al. [14] prepared PtRu electrodes with different compositions (Pt:Ru atomic ratios between 1:0.087 and 1:0.61) to study the electro-oxidation of ethylene glycol in acid medium. They observed that the catalytic activity increased with the ruthenium content; however, electrodes with higher ruthenium content could not be prepared by this methodology.

In this work PtRu/C and PtSn/C electrocatalysts with Pt:Me atomic ratios between 1:3 and 3:1 were prepared by alcohol-reduction process [15, 16] and tested for ethylene glycol oxidation at room temperature using the thin porous coating technique [10, 17].

2. Experimental

PtRu/C and PtSn/C electrocatalysts were prepared using H₂PtCl₆·6H₂O (Aldrich), RuCl₃·xH₂O (Aldrich) and SnCl₂·2H₂O (Aldrich) as metal sources, ethylene glycol (Merck) as solvent and reducing agent and Carbon Vulcan XC72R as support [15, 16].

The Pt:Ru and Pt:Sn atomic ratios were obtained by EDAX analysis using a scanning electron microscope

Philips XL30 with a 20 keV electron beam and provided with EDAX DX-4 microanalyser.

The XRD analyses were performed using a Rigaku diffractometer model Multiflex with a $\text{CuK}\alpha$ radiation source.

Transmission electron microscopy (TEM) was carried out using a Carl Zeiss CEM 902 apparatus with a Proscan high-speed slow-scan CCD camera and digitalized (1024×1024 pixels, 8 bits) using the AnalySis software. The particle size distributions were determined by measuring the nanoparticles from micrographs using Image Tool Software.

Electrochemical studies of the electrocatalysts were carried out using the thin porous coating technique [10, 17]. An amount of 20 mg of the electrocatalyst was added to a solution of 50 ml of water containing 3 drops of a 6% polytetrafluoroethylene (PTFE) suspension. The resulting mixture was treated in an ultrasound bath for 10 min, filtered and transferred to the cavity (0.30 mm deep and 0.36 cm^2 area) of the working electrode. The quantity of electrocatalyst in the working electrode was determined with a precision of 0.0001 g. In cyclic voltammetry and chronoamperometry experiments the current values (I) were expressed in amperes and were normalized per gram of platinum ($A \text{ g Pt}^{-1}$). The quantity of platinum was calculated considering the mass of the electrocatalyst present in the working electrode multiplied by its percentage of platinum (Table 1). The reference electrode was a RHE and the counter electrode was a platinized Pt plate. Electrochemical measurements were made using a Microquimica (model MQPG01, Brazil) potentiostat/galvanostat coupled to a personal computer and using the Microquimica software. Cyclic Voltammetry was performed in a 0.5 mol l^{-1} H_2SO_4 solution saturated with N_2 . The evaluation of ethylene glycol oxidation was performed at 25 °C in three different concentrations: 0.1, 0.5 and 1.0 mol l^{-1} . For comparative purposes a commercial carbon supported PtRu catalyst from E-TEK (20 wt. %, Pt:Ru molar ratio 1:1, Lot # 3028401) was used. For chronoamperometry, the electrolyte solution was 1 mol l^{-1} of ethylene glycol in 0.5 mol l^{-1} H_2SO_4 .

Table 1. Pt:Me atomic ratio (from EDAX) and particle sizes (from TEM) of the prepared electrocatalysts

Electrocatalyst	Pt /wt. %	Me /wt. %	Pt:Me atomic ratio	Pt:Me atomic ratio EDAX	Particle size /nm
PtRu/C 1:1	13.2	6.8	1:1	1:1.1	4.0 ± 1.5
PtRu/C 1:3	7.8	12.2	1:3	1:2.5	5.5 ± 2.0
PtRu/C 3:1	17.0	3.0	3:1	3:1	5.0 ± 1.5
PtSn/C 1:1	12.4	7.6	1:1	1.2:1	4.0 ± 1.0
PtSn/C 1:3	7.1	12.9	1:3	1:2.5	5.0 ± 1.5
PtSn/C 3:1	16.6	3.4	3:1	2.5:1	–
PtRu/C E-TEK	13.2	6.8	1:1	1:1.1	2.5 ± 0.7

3. Results and discussion

The carbon-supported platinum–ruthenium and platinum–tin nanoparticles were prepared in a single step (co-reduction of mixed ions) using ethylene glycol as solvent and reducing agent in the presence of carbon Vulcan XC72R [15, 16]. The Pt:Ru and Pt:Sn atomic ratios of the obtained electrocatalysts were similar to the atomic ratios used in the preparations (Table 1). The X-ray diffractograms of the electrocatalysts are shown in Figure 1. For all PtRu/C electrocatalysts the first broad peak at about 25° is associated with the Vulcan XC-72R support material. The diffractograms of PtRu/C electrocatalysts with a Pt:Ru molar ratio of 3:1 and 1:1 show peaks at approximately $2\theta=40^\circ$, 47° , 67° and 82° that are associated with the (111), (200), (220) and (311) planes, respectively, of the fcc structure of platinum and characteristic of PtRu alloys with up to 50 at.% of ruthenium [16]. The electrocatalyst PtRu/C with a Pt:Ru molar ratio of 1:3 shows the typical peaks of the fcc structure of platinum with a shoulder at about 44° corresponding to a metallic ruthenium or to materials rich in Ru with hexagonal structure [17]. The PtSn/C electrocatalysts with a Pt:Sn atomic ratio of 3:1 and 1:1 also show four diffraction peaks at about $2\theta=40^\circ$, 47° , 67° and 82° characteristic of the fcc structure of platinum and platinum alloys. Recently, Xin et al. [18] prepared PtSn/C electrocatalyst with a Pt:Sn atomic ratio of 2:1 by a similar procedure. The analysis of the diffractogram also revealed the typical peaks relative to the fcc structure of platinum. The comparison to the lattice parameter of bulk platinum showed that the addition of Sn increases the lattice parameter, indicating a Pt and Sn alloy to some extent [18]. Interestingly, the typical peaks relative to the fcc structure of platinum are not evident for PtSn/C electrocatalyst with a Pt:Sn atomic ratio of 1:3. The diffractogram of this sample shows peaks at about $2\theta=27^\circ$, 34° , 52° , 54° , 62° and 66° that are associated with the planes (110), (101), (211), (220), (310) and (301), respectively, and characteristic of

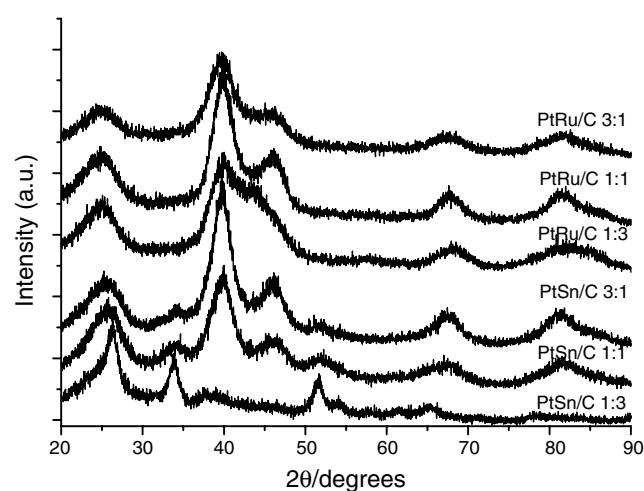


Fig. 1. X-ray diffractograms of PtRu/C and PtSn/C electrocatalysts.

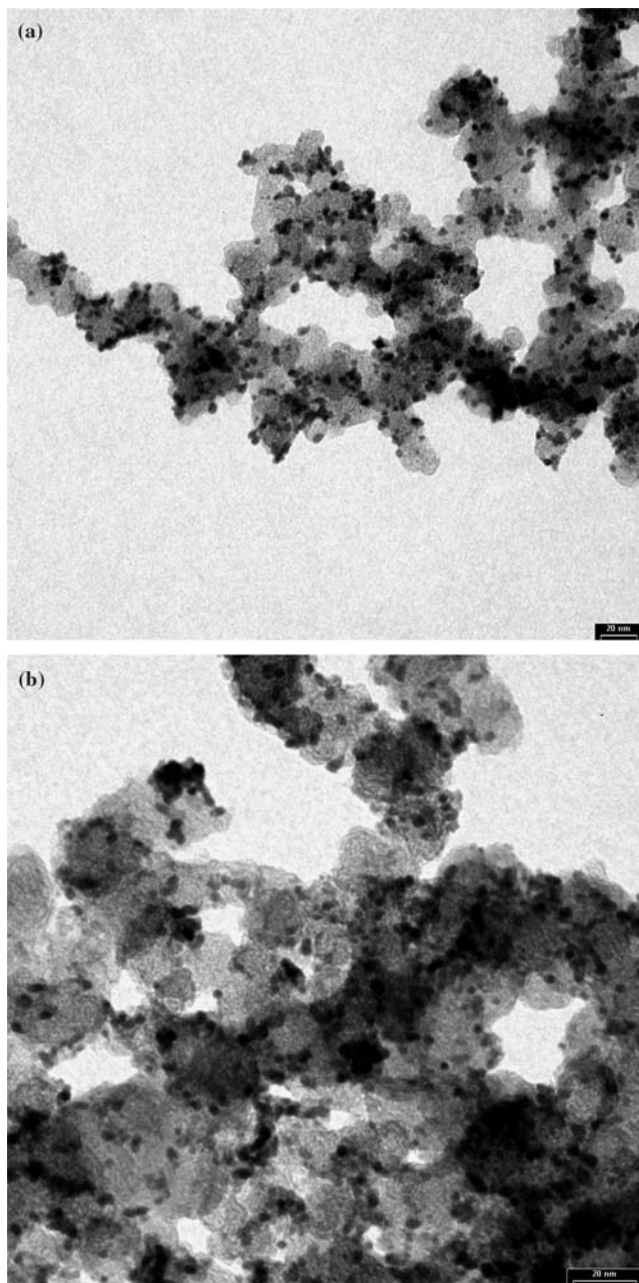


Fig. 2. TEM micrographs (a) PtRu/C 1:1 and (b) PtSn/C 1:1 electrocatalysts.

cassiterite SnO_2 phase [19]. The peaks of cassiterite phase ($2\theta=34^\circ$ and 52°) are also present in the diffractograms of PtSn/C electrocatalysts with a Pt:Sn atomic ratio of 3:1 and 1:3. The TEM micrographs of PtRu/C electrocatalysts (Figure 2a) show the nanoparticles with a good distribution on the carbon support and particle sizes in the range 4–5 nm [16]. PtSn electrocatalysts (Figure 2b) have similar particle sizes; however, the nanoparticle distribution on the carbon is not as good as observed for PtRu/C electrocatalysts.

Cyclic voltammograms for the PtRu/C and PtSn/C electrocatalysts with different atomic ratios, in the absence of ethylene glycol, are shown in Figures 3a and 3b, respectively. In this case, all the electrocatalysts

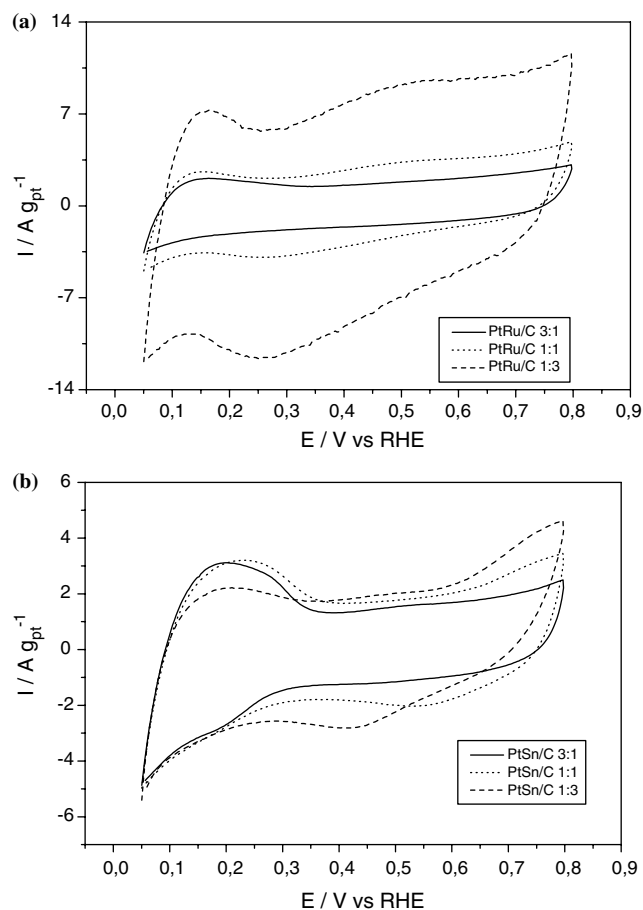


Fig. 3. Cyclic voltammetry of (a) PtRu/C and (b) PtSn/C electrocatalysts in $0.5 \text{ mol l}^{-1} \text{ H}_2\text{SO}_4$ with a sweep rate of 10 mV s^{-1} .

do not have a well-defined hydrogen adsorption–desorption region and the currents in the double layer increase with increase in ruthenium and tin content. This may be attributed to the presence of more ruthenium and tin oxide species, which are very important to methanol, ethanol and ethylene glycol oxidation at low potentials [14, 20–23].

The electro-oxidation of ethylene glycol was studied varying the concentration from 0.1 to 1.0 mol l^{-1} (Figure 4). In a general manner, for all electrocatalysts, the current values in the hydrogen region (0 – 0.4 V) decrease with increase in ethylene glycol concentration, most likely due to the increase in ethylene glycol adsorption on the nanoparticles surface [20, 21]. For potentials more positive than 0.4 V the current values increase with ethylene glycol concentration even for 1.0 mol l^{-1} .

The PtRu/C and PtSn/C electrocatalysts performances in ethylene glycol oxidation are shown in Figures 5a and 5b, respectively. In these figures the anodic cyclic voltammetry responses were plotted after subtracting the background currents [10, 17] and the current values were normalized per gram of platinum, considering that ethylene glycol adsorption and dehydrogenation occur only on platinum sites at ambient temperature [24–27]. The electro-oxidation of ethylene

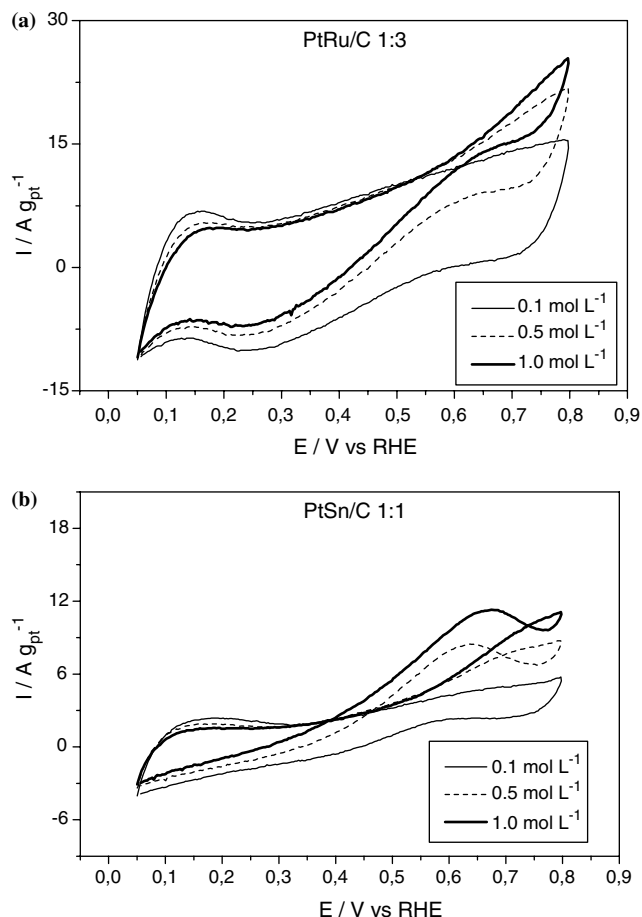


Fig. 4. Cyclic voltammety of (a) PtRu/C 1:3 and (b) PtSn/C 1:1 electrocatalysts in $0.5 \text{ mol l}^{-1} \text{ H}_2\text{SO}_4$ containing different concentrations of ethylene glycol with a sweep rate of 10 mV s^{-1} .

glycol in the presence of PtRu/C electrocatalysts only starts above 0.4 V . The PtRu/C electrocatalysts with a Pt:Ru atomic ratio of 1:1 and 3:1 give poorer performance than the commercial PtRu/C E-TEK electrocatalyst, while the electrocatalyst with a Pt:Ru atomic ratio of 1:3 shows a better performance than the commercial electrocatalyst above 0.5 V . Vielstich et al. [14] studied the electro-oxidation of ethylene glycol in acid medium using PtRu electrodes prepared by electrodeposition and observed that the performances increased with increase in ruthenium content. In that study, *in situ* FTIR spectroscopy was used to monitor the reaction products, showing that the dissociative adsorption of ethylene glycol produces as intermediate adsorbed carbon monoxide. Besides CO_2 , glycolic and/or oxalic acid were observed as soluble products. Contrary to expectation, as in the case of methanol where the oxidation of the CO intermediate to CO_2 is improved in the presence of ruthenium, the product analysis showed that the complete oxidation of ethylene glycol to CO_2 was favored by a high platinum content. It was suggested that the dissociative adsorption of ethylene glycol was unfavorable in the presence of ruthenium and that ruthenium promotes not only the oxidation of CO to CO_2 , but also parallel pathways, which require oxygen donor species for product formation [14].

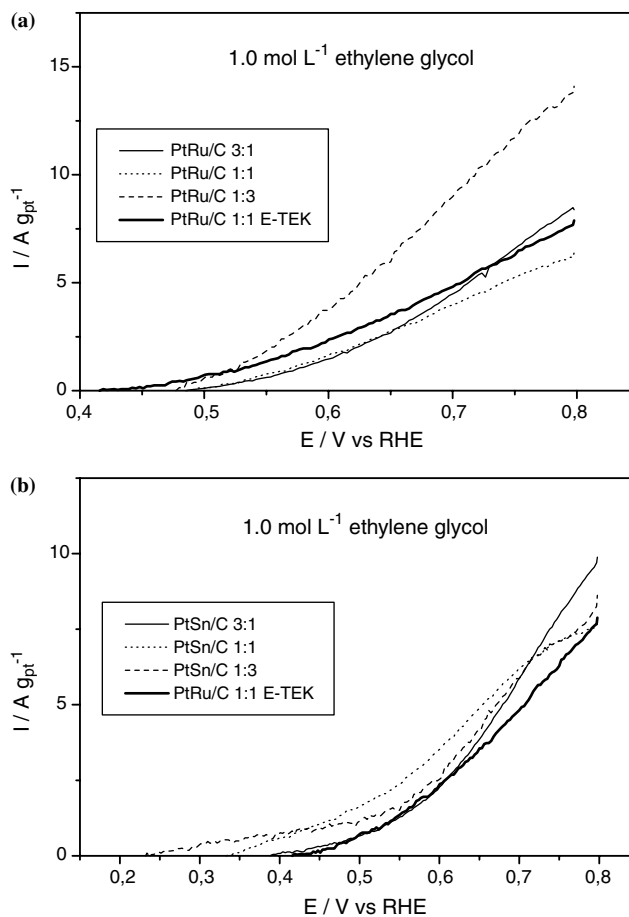


Fig. 5. Cyclic voltammety of (a) PtRu/C and (b) PtSn/C electrocatalysts in $0.5 \text{ mol l}^{-1} \text{ H}_2\text{SO}_4$ containing 1.0 mol l^{-1} of ethylene glycol with a sweep rate of 10 mV s^{-1} , considering only the anodic sweep.

PtSn/C electrocatalysts showed better performance than the commercial PtRu/C electrocatalyst for ethylene glycol electro-oxidation (Figure 5b). In addition, the electro-oxidation of ethylene glycol with PtSn/C electrocatalysts starts at lower potentials than PtRu/C electrocatalysts and a desirable decrease in these values was observed with increase in tin content. For instance, the electro-oxidation starts at approximately 0.25 V for the electrocatalyst with a Pt:Sn molar ratio of 1:3. The electrocatalysts with more tin content (Pt:Sn molar ratio of 1:1 and 1:3) showed better performance than those (Pt:Sn molar ratio of 3:1) with higher platinum content. Similar behavior was observed by Xin et al. [22, 23] in a single direct ethanol fuel cell. The PtSn/C electrocatalysts with a Pt:Sn atomic ratio of 1:1, 1.5:1 and 2:1 showed better performance than those with 3:1 and 4:1 and all of them were more active than the PtRu/C electrocatalyst with a Pt:Ru atomic ratio of 1:1. The better performance of PtSn/C electrocatalysts in ethanol oxidation was attributed to changes in the platinum lattice due to the addition of tin and to the electronic interaction between Pt and Sn, both of which favor C-C bond cleavage, while the CO intermediate formed during breaking of the C-C bond was removed by tin oxide species (bifunctional mechanism) [22, 23].

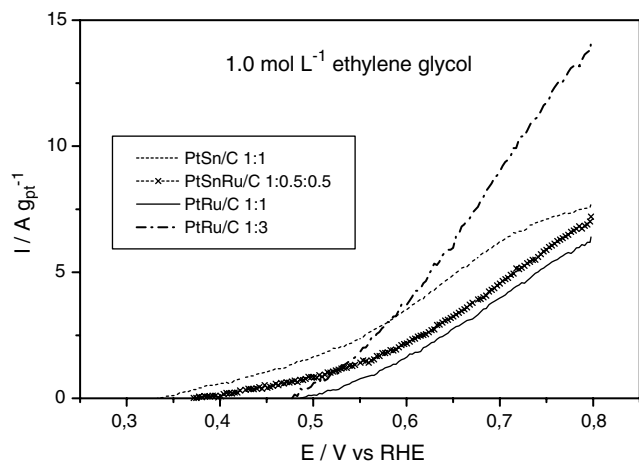


Fig. 6. Cyclic voltammetry of PtSn/C 1:1, PtSnRu/C 1:0.5:0.5, PtRu/C 1:1 and PtRu/C 1:3 electrocatalysts in $0.5 \text{ mol l}^{-1} \text{ H}_2\text{SO}_4$ containing 1.0 mol l^{-1} of ethylene glycol with a sweep rate of 10 mV s^{-1} , considering only the anodic sweep.

The performances of PtRu/C (Pt:Ru atomic ratio of 1:1 and 1:3), PtSn/C (Pt:Sn atomic ratio of 1:1) and PtSnRu/C (Pt:Sn:Ru atomic ratio of 1:0.5:0.5) electrocatalysts for ethylene glycol electro-oxidation are shown in Figure 6. The performance of the PtSnRu/C 1:0.5:0.5 electrocatalyst was better than that of PtRu/C 1:1 but inferior that of PtSn/C 1:1 electrocatalyst, which presents the best performance in the region of interest for direct alcohol fuel cell applications (0.2–0.6 V). The PtRu/C 1:3 electrocatalyst showed a superior performance but only above 0.6 V. The current-time curves for PtSn/C 1:1 and PtRu/C 1:3 electrocatalysts are shown in Figure 7. In all of the current-time curves there is an initial current drop in the first 5 min, followed by a slower decay. The current values for PtSn/C 1:1 electrocatalyst are always higher than those obtained for PtRu/C 1:3 electrocatalyst.

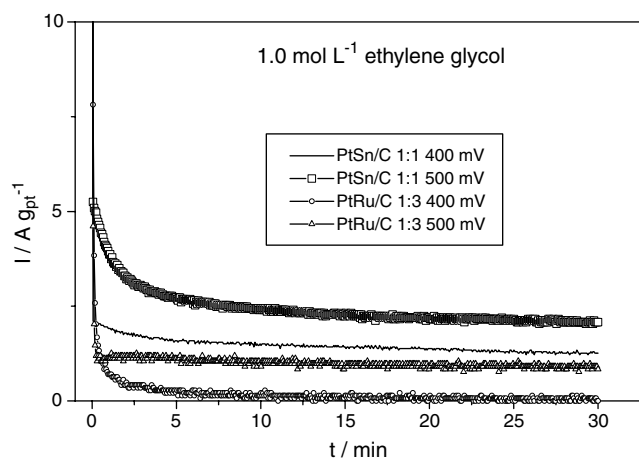


Fig. 7. Current-time curves at 0.4 and 0.5 V in 1 mol l^{-1} ethylene glycol solution in $0.5 \text{ mol l}^{-1} \text{ H}_2\text{SO}_4$ for PtRu/C 1:3 and PtSn/C 1:1 electrocatalysts.

4. Conclusions

The alcohol-reduction process was an effective method for making active PtRu/C and PtSn/C electrocatalysts for ethylene glycol oxidation. The electrocatalysts prepared with a Pt:Me molar ratio of 3:1 and 1:1 show the typical fcc structure of platinum and platinum alloys. Increase in ruthenium and tin content (Pt:Me molar ratio of 1:3) leads to the formation of a separated ruthenium and tin oxide phase, respectively. For PtRu/C electrocatalysts the electro-oxidation of ethylene glycol starts at lower potentials and the current values increase with the increase in ruthenium content. In the presence of PtSn/C electrocatalysts the electro-oxidation also starts at lower potentials with increase in tin content; however, in the region between 0.4 and 0.6 V the electrocatalyst with a Pt:Sn atomic ratio of 1:1 shows higher current values than the electrocatalyst with an atomic ratio of 1:3. Independent of the Pt:Me atomic ratio used, PtSn/C electrocatalysts are better for ethylene glycol oxidation than PtRu/C electrocatalysts because the oxidation starts at lower potentials and high current values are obtained in the region of interest for direct alcohol fuel cells. However, in the presence of platinum and tin oxide species, a detailed study is needed in order to know if the adsorption of ethylene glycol occurs with breaking of C–C bond and formation of CO as intermediate, which is oxidized to CO_2 (bifunctional mechanism), or if the dissociative adsorption is unfavorable and these species leads to the formation of partial oxidized products like aldehydes and acids.

Acknowledgements

The authors thank Fundação de Amparo à Pesquisa do Estado de São Paulo – FAPESP for financial support.

References

1. E.R. Gonzalez, *Quim. Nova* **23** (2000) 262.
2. H. Wendt, M. Linardi and E.M. Arico, *Quim Nova* **25** (2002) 470.
3. H. Wendt, M. Götz and M. Linardi, *Quim. Nova* **23** (2000) 538.
4. L. Carrette, K.A. Friedrich and U. Stimming, *Fuel Cells* **1** (2001) 5.
5. C. Lamy, A. Lima, V. LeRhun, F. Delime, C. Coutanceau and J.-M. Léger, *J. Power Sources* **105** (2002) 283.
6. S. Wasmus and A. Kuver, *J. Electroanal. Chem.* **461** (1999) 14.
7. A. Heinzl and V.M. Barragán, *J. Power Sources* **84** (1999) 70.
8. T. Iwasita, *Electrochim. Acta* **47** (2002) 3663.
9. F. Vigier, C. Coutanceau, A. Perrard, E.M. Belgsir and C. Lamy, *J. Appl. Electrochem.* **34** (2004) 439.
10. A. Oliveira Neto, M.J. Giz, J. Perez, E.A. Ticianelli and E.R. Gonzalez, *J. Electrochem. Soc.* **149** (2002) A272.
11. E. Peled, T. Duvdevani, A. Ahron and A. Melman, *Electrochem. Solid-State Lett.* **4** (2001) A38.
12. E. Peled, V. Livshits and T. Duvdevani, *J. Power Sources* **106** (2002) 245.
13. A. Kelaidopoulou, E. Abelidou, A. Papoutsis, E.K. Polychroniadis and G. Kokkinidis, *J. Appl. Electrochem.* **28** (1998) 1101.

14. R.B.Lima, V.Paganin, T.Iwasita and W. Vielstich, *Electrochim. Acta* **49** (2003) 85.
15. E.V. Spinacé, A.O. Neto, T.R.R. Vasconcelos and M. Linardi, Brazilian Patent INPI-RJ, PI0304121-2, 2003.
16. E.V. Spinacé, A.O. Neto, T.R.R. Vasconcelos and M. Linardi, *J. Power Sources* **137** (2004) 17.
17. F. Colmati Jr., W.H. Lizcano-Valbuena, G.A. Camara, E.A. Ticianelli and E.R. Gonzalez, *J. Braz. Chem. Soc.* **13** (2002) 474.
18. L. Jiang, G. Sun, Z. Zhou, W. Zhou and Q. Xin, *Catal. Today* **93-95** (2004) 665.
19. W.S. Cardoso, M.S.P. Francisco, A.M.S. Lucho and Y. Gushiken, *Solid State Ionics* **167** (2004) 165.
20. E.V. Spinacé, A.O. Neto and M. Linardi, *J. Power Sources* **124** (2003) 426.
21. E.V. Spinacé, A.O. Neto and M. Linardi, *J. Power Sources* **129** (2004) 121.
22. W. Zhou, Z. Zhou, S. Song, W. Li, G. Sun, P. Tsiakaras and Q. Xin, *Appl. Catal. B Environ.* **46** (2003) 273.
23. W.J. Zhou, B. Zhou, W.Z. Li, Z.H. Zhou, S.Q. Song, G.Q. Sun, Q. Xin, S. Douvartzides, M. Goula and P. Tsiakaras, *J. Power Sources* **126** (2004) 16.
24. H.A. Gasteiger, N. Markovic, P.N. Ross and E.J. Carins, *J. Electrochem. Soc.* **141** (1994) 1795.
25. S.Lj. Gojkovic, T.R. Vidakovic and D.R. Durovic, *Electrochim. Acta* **48** (2003) 3607.
26. M. Christov and K. Sundmacher, *Surf. Sci.* **547** (2003) 1.
27. L. Dubau, F. Hahn, C. Countaceau, J-M. Leger and C. Lamy, *J. Electroanal. Chem.* **554-555** (2003) 407.